Ion-Mediated Ligand Exchange and Size-Focusing Of Semiconductor Nanocrystals in Ligand-Saturated Solutions.

Natalia Kholmicheva[1,2], Mingrui Yang[1,2], Pavel Moroz[1,2], Holly Eckard[3], Abigail Vore[3], James Cassidy[1,3], Mariia Pushina[1,3], Anthony Boddy[3], Dmitry Porotnikov[1,2], Pavel Anzenbacher[1,3], Mikhail Zamkov[1,2].*

The Center for Photochemical Sciences[1], Department of Physics[2] and Department of Chemistry[3]

Bowling Green State University, Bowling Green, Ohio 43403.

Corresponding author: zamkovm@bgsu.edu; Tel: 419-372-0264; Fax: 419-372-9938

RECEIVED DATE (to be automatically inserted after your manuscript is accepted if required)

Abstract. Controlling the morphology of colloidal semiconductor nanocrystals (NCs) remains to be a challenging task. Traditional growth strategies employ a high concentration of monomers to promote particle nucleation, which tends to oversaturate the solution with reactive species. This leads to secondary nucleation events and other dispersion-broadening processes. Here, we explore monomer-deprived synthetic conditions as a bilateral strategy for tuning both the shape

and the surface-ligand chemistry of semiconductor colloids. Rather than controlling the nucleation phase, the present method employs a post-synthetic treatment based on low-temperature digestive ripening (DR), where small particles grow at the expense of larger ones. The feasibility of the present approach was demonstrated by observing a four-fold reduction in the CdSe nanoparticle size dispersion during the digesting ripening reaction, which was induced by high concentrations of L-type (amines) or X-type (oleic acid) ion-solubilizing ligands. In the latter case, a classically forbidden L→X ligand exchange was enabled by the concurrent process of the surface ion diffusion. The size-focusing capabilities of the technique were subsequently demonstrated by ripening ZnSe NCs, which shape homogeneity is generally difficult to achieve.

INTRODUCTION

Colloidal semiconductor nanocrystals (NCs) have attracted considerable attention as possible candidates for developing a wide variety of optoelectronic materials.[1,2] The potential benefits of colloidal semiconductors arise from introducing a strong carrier confinement regime to applications in solid state lighting,[3,4] photovoltaics,[5-67] bio sensing,[8,9] and catalysis.[10,11] In many of these areas, the sample homogeneity plays an important role as a defining aspect of the excited state energetics.[12-14] The synthetic control over the morphology of colloidal semiconductor nanocrystals, however, remains difficult to achieve.[15-22]

Primary factors underlying a broad distribution of particle sizes associated with a colloidal synthesis have been the subject of many investigations.[16,20,23-27] According to the general consensus, nanoparticle growth processes that are non-linear with the monomer concentration, represent the leading cause of the ensuing shape inhomogeneity.[28] One of such processes is the nanoparticle burst nucleation that, according to model predictions,[29] leads to the spontaneous formation of highly polydispersed seeds before the size-focusing regime associated with the concentration-dependent monomer diffusion and Ostwald ripening[30] takes place. Even

during the post-nucleation stage, delayed nucleation continues to compete with the homogenous nanoparticle growth (Finke-Watzky mechanism)[31] until monomers are depleted.[32] The dispersion-broadening nucleation processes, however, can be avoided thought the application of post synthetic treatments that do not employ precursors.[33,34] Along these lines, digestive ripening (DR) has been widely used for reducing the shape dispersion of metal nanoparticles.[35-40] During the DR treatment, small particles grow at the expense of larger ones, in a manner that defies the classical Gibbs–Thomson mechanism[29] of nanoparticle ripening based on the reduction of the interfacial free energy. Recently, the digestive ripening treatment has also been applied to semiconductor nanocrystals[41] resulting in a unique particle shape evolution at high reaction temperatures that was not previously reported for metal colloids. It was observed that above a material-specific thermal threshold, the DR treatment of semiconductor NCs caused a significant coalescence-driven nanocrystal growth. Conversely, it was hypothesized that at reaction temperatures below the coalescence threshold, size focusing could become the sole ripening process. Along these lines, the present work explores the low-temperature DR regime as a potential strategy for reducing the dispersion of nanoparticle sizes in semiconductor colloids.

Here, we explore the low-temperature digestive ripening of semiconductor nanocrystals as a post synthetic strategy for reducing the particle size dispersion in colloidal solutions. The absence of precursors in the DR reaction mixture allows suppressing non-linear nucleation processes, thus giving it a certain advantage over single-step hot injection and heat-up synthetic strategies. In present experiments, the size focusing reaction was initiated by introducing a high concentration of free ligands to nanoparticle solutions, which enhanced the rate of ion and neutral monomer diffusion at the nanocrystal-solvent interface. At elevated solvent temperatures, this resulted in a homogenous redistribution of desorbed ions and monomers across a colloidal

sample leading to the reduction in the nanoparticle size dispersion. The feasibility of the size focusing effect was investigated by using a mixture of two CdSe NC samples featuring different particle diameters as a model system of a polydisperse nanoparticle population. In the course of the digestive ripening treatment, the two CdSe sizes have gradually converged into one corresponding to the four-fold reduction in the particle size dispersion. The size focusing reaction was found to be similarly effective when initiated using either L-type (oleylamine) or X-type (oleic acid) free ligands. The technique was subsequently adapted to achieve size focusing in samples of ZnSe NCs, where the shape homogeneity is notoriously difficult to achieve. One of the unexpected outcomes of size-focusing experiments was the observation that digestive ripening enabled complex ligand exchange processes that required restructuring of nanocrystal surfaces. In particular, the digestive ripening treatment has been shown to promote a classically forbidden L → X ligand exchange[42] in CdSe NCs, which was made possible due to the desorption of surface Se, mediated by ligand saturated . Overall, we expect that the demonstrated strategy can be utilized as a simple post synthetic procedure for controlling the surface chemistry and reducing the particle size dispersion of semiconductor colloids.

METHODS

Materials. The following materials were used: cadmium oxide (CdO, 99% STREM), 1-octadecene (ODE, 90% Aldrich), n-octadecylphosphonic acid (ODPA, PCI), octadecylamine (ODA, 90%, Acros), oleic acid (OA, 90% Aldrich), sulfur (S, 99.99% Acros), methanol (anhydrous, 99.8% Aldrich), chloroform (anhydrous, 99% Aldrich), oleylamine (OLAM, tech., 70% Aldrich), hexane (anhydrous, 95% Aldrich), ethanol (anhydrous, 95% Aldrich), tri-n-octylphosphine (TOP, 97% STREM), tri-n-octylphosphine oxide (TOPO, 99.0% Aldrich), selenium powder (Se, 200 mesh, Acros), acetone (anhydrous, Amresco, ACS grade), stearic acid

(97% Aldrich), tributylphosphine (TBP, 97% Aldrich) and diethylzinc (95% STREM). All reactions were performed under argon atmosphere using the standard Schlenk technique. The centrifuge used for precipitation operated at 5400 and 7200 rpm.

Synthesis of CdSe NCs with $\lambda_{exciton}$ = 470nm - 520nm. Small-diameter CdSe NCs were fabricated according to a previously reported procedure.[43] Briefly, TOPO (3.0 g), ODPA (0.280 g), and CdO (0.060 g) were mixed in a 50 mL flask, heated to 150°C and exposed to vacuum for 1 hour. Then, under argon, the solution was heated to 300°C to dissolve CdO until the mixture turned optically clear and colorless. At this point, 1.5 g of TOP was injected into the flask and the temperature was raised to 330 ºC. The reaction flask with Cd precursor was raised up from the heating mantle right before the injection of Se precursor to get small-diameter nanoparticles. A selenium precursor prepared by dissolving 0.060 g of Se in 1 mL of TOP through heating to 150 ºC under argon and cooling to room temperature was injected all at once into the raised flask (at 330 ºC). After the synthesis, nanocrystals were precipitated with ethanol, and washed by repeated redissolution in chloroform and precipitation with the addition of ethanol. Finally, the product was stored in chloroform (3 ml).

Synthesis of CdSe NCs with $\lambda_{exciton}$ = 560nm - 580nm. Large-diameter CdSe NCs were synthesized using a previously reported technique.[44] In a three-neck flask, a mixture of stearic acid (0.23 g), ODE (2.54 mL), and CdO (0.026 g) was heated to 200 °C under argon atmosphere until the solution turned clear indicating the formation of cadmium stearate. Subsequently, the reaction mixture was cooled to room temperature, at which point 1.5 g of ODA and 0.5 g of TOPO were added. The flask was reheated to 260 °C under vigorous stirring and selenium solution, prepared under argon by dissolving 0.158 g of selenium powder *via* sonication in TBP (0.58 mL) and ODE (1.70 mL) mixture, was quickly injected. The temperature was set to 250 °C and the reaction continued until the desired size of nanocrystals was reached. The reaction was quenched by removing the flask from the heating mantle. Once the flask's contents had cooled to 60°C, chloroform (10 mL) was injected into the flask to prevent solidification. To remove the unreacted material, the contents of the flask were centrifuged, and the precipitate was discarded. Acetone (6 mL) was added to the supernatant, and the solution was centrifuged again. The final precipitate was redispersed in chloroform (3 ml).

Synthesis of ZnSe NCs. Synthesis of ZnSe NCs was adapted from Cozzoli et al.[45] Briefly, 7 g of ODA was degassed under vacuum at 130°C for 1 h and subsequently heated to 315 °C under argon flow. Se precursor was prepared by mixing 0.063 g of Se powder in 2 mL of TOP followed by degassing at 120°C for 1 h and injecting it into ODA solution. An amount of 1 mL of diethylzinc was injected into the reaction mixture at 315 °C. Upon injection, the temperature dropped to 265 °C and was maintained at this level throughout the entire synthesis. The reaction was stopped after 4 min when the desired particle size was reached. Nanocrystals were precipitated with methanol and redispersed in chloroform.

Digestive Ripening Protocol. Nanocrystal seeds in hexane (either CdSe or ZnSe NCs) were transferred to a flask containing a mixture of coordinating ligands (OLAM or OA) and ODE. The mixture was then degassed at 120°C to remove hexane. The ratio of ligand to solvent (ODE) molecules varied from 60:40 to 100:0 depending on the experiment, while the total volume of the reaction mixture was kept the same, around 7ml. To initiate digestive ripening, the temperature of the flask was raised to 150-180°C under argon atmosphere. The reaction was stopped by removing the flask from the heating mantle and NCs were separated from the solution by precipitation with acetone or ethanol and redispersed in hexane.

Characterization. UV-vis absorption spectra were recorded using a CARY 60 scan spectrophotometer. High resolution transmission electron microscopy (TEM) measurements were carried out using JEOL 311UHR operated at 300 kV. Specimens were prepared by depositing a drop of NP solution in organic solvent onto a carbon-coated copper grid and allowing it to dry in air. Powder X-Ray diffraction measurements were carried out with a Bruker D8 Advance PXRD. Energy dispersive X-ray (EDX) analysis was performed using Hitachi 2700 operated at 20 kV. Proton NMR (^{1}H-NMR) spectra were recorded on Bruker Avance III spectrometer at 500 MHz at 298 K. Proton NMR chemical shifts (δ) are reported in parts per million (ppm) relative to residual solvent signals in $CDCl_3$ (δ = 7.26). The emission quantum yield of CdSe NC samples was determined relative to a Cy3 dye.

RESULTS AND DISCUSSION

Classically, digestive ripening is believed to be driven by the ligand-mediated dissolution of larger nanoparticles in favor of smaller ones and is often considered to be the opposite of Ostwald ripening.[30] Several studies have investigated the mechanistic aspects of digestive ripening in metal colloids,[46-4849] concluding that the presence of free ligand molecules in the reaction mixture allows dissolving surface ions into the solution, which subsequently get re-adsorbed by other colloids. Such a diffusive exchange of ions between metal nanoparticles leads to the reduction in the particle size dispersion. In the case of semiconductor NCs, the DR process was shown to exhibit two distinct temperature regimes distinguished by a rather sharp thermal transition (e.g. $T_{th} \approx 220$ ˚C for CdS NCs).[32] Above the thermal threshold, an average particle size in the sample was found to increase as a result of coalescence. This process was accompanied by the concurrent size focusing due to ion and monomer diffusion, which ultimately resulted in the formation of large-diameter uniform nanocrystals (e.g. 18.1-nm CdS NCs featuring $\Delta d/d < 3\%$).[41] Based on these findings, it was reasonable to assume[50] that below the critical temperature for coalescence, one can expect to see a reduction in the size dispersion without significant changes in the average particle diameter.

As a model system of a polydisperse nanoparticle sample, we have employed a mixture of the two different-diameter CdSe NCs (d = 2.1 and d = 2.6 nm) exhibiting a corresponding sample size dispersion of 22%. Both nanoparticle types were prepared by means of traditional hot-injection routes[43,44] that can result in three different types of surface ligands, including cadmium carboxylate $Cd(O_2CR)_2$, phosphine (PR_3) complexes,[51] and X-type acids (oleic, phosphonic, or steric acids) donating one electron to a cadmium bond. The presence of L-type phosphine passivation in investigated samples was partly supported by the fact that the exposure

of as-prepared CdSe colloids to a concentrated solution of $Cd(O_2CR)_2$ produced a 3-5 nm red-shift of the exciton absorption, indicating the presence of surface Se sites that are coordinated to Cd-L complexes.

The absorption profile of the $CdSe_{470}$-$CdSe_{520}$ mixture in Fig. 1a (bottom black curve) exhibits distinguishable excitonic features of the smaller and larger species corresponding to average particle sizes[52] of 2.1 and 2.6 nm, respectively. The presence of the two different particle sizes is also evident in the photoluminescence spectrum of the mixed sample (Fig. SF1) as well as in the transmission electron microscopy (TEM) image of the mixture (Fig. SF2). To initiate digestive ripening, a mixed-diameter sample was transferred to a reaction flask containing 60% of OLAM ligands by volume and heated to about 150-180 ˚C. This temperature interval represents the low-temperature range where the processes of interparticle coalescence are suppressed (see Ref. 41). During the DR treatment, the particle size evolution was then monitored through the changes in the absorption profile, as shown in Fig.1b.

Figure 1 summarizes the DR dynamics of a mixed-diameter sample containing two CdSe NC types in a OLAM:ODE = 60:40 mixture. During a ≈ 14-hour DR treatment at temperatures not exceeding 180 ˚C, the lowest-energy excitonic features of the two nanoparticle types appear to gradually converge into a single-particle profile, indicating the reduction in the sample size dispersion. The spectral position of the $1S_{3/2}(h)1S(e)$ transition in the final product corresponds to a particle diameter of about 2.45 nm,[52] which is close to the expected volume-weighted average of the original sizes in the mixture ($\bar{d} \approx \sqrt{d_1^3 + d_2^3}/2 = 2.37$ nm). Notably, the total concentration of CdSe nanoparticles in the flask did not appear to change significantly, such that processes of precipitation or dissolution of nanocrystals during the digestive ripening reaction were deemed minimal. The crystal structure of CdSe NCs was also found to be preserved during the DR treatment (see XDR analysis in Fig. SF3) consistent with the absence of phase-changing

coalescence processes.[41] The size dispersion analysis indicates the reduction in the standard deviation of particle diameters from 22% in the original sample to about 5% in the final product.

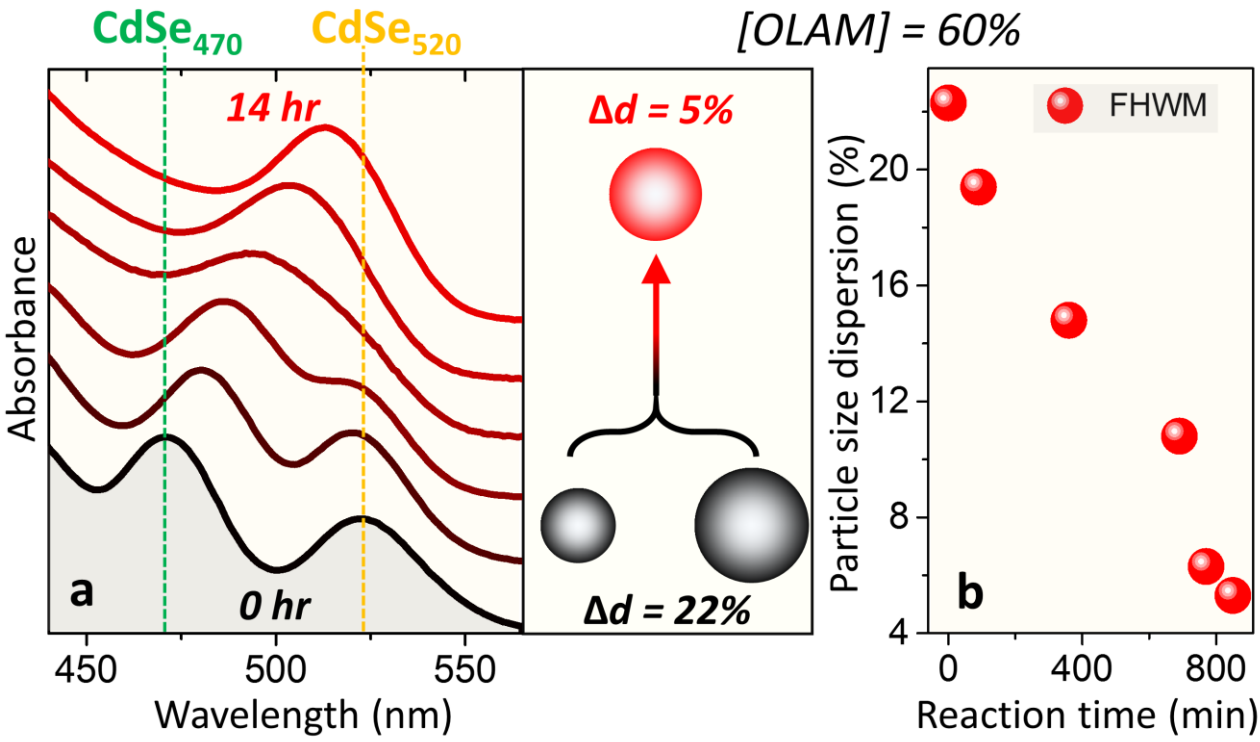

Figure 1. (a). OLAM-induced digesting ripening of a CdS_{470} + $CdSe_{520}$ nanocrystal mixture containing two sizes of CdSe nanocrystals (d = 2.1 nm and d = 2.6 nm, respectively). The associated low-energy absorbing transitions are labelled as green and yellow dashed lines. Heating of the polydisperse nanoparticle sample in the OLAM:ODE = 60:40 reaction mixture at T = 150-180 ˚C results in the gradual convergence of the two absorbing features into one, corresponding to the reduction in the particle size dispersion from 22% to about 5%. (b). The corresponding evolution of the FWHM for the combined 1S(e)1S(h) absorption feature in a mixed-diameter CdSe NC sample with the DR reaction time.

In addition to size focusing, digestive ripening of CdSe NCs was accompanied by the enhancement in PL lifetimes (Fig. 2c) corresponding to a 4% → 38% increase in the emission quantum yield (QY). This trend was consistent with previous reports of the increased PL

intensity in phosphonate- or cadmium carboxylate-capped CdSe NC upon the displacement of original ligands with amines.[20,24,53-55] For instance, Talapin et al.[24] has reported an emission QY = 50% for CdSe NCs exposed to a high concentration of alkylamines at 240 ˚C. Another study corroborated this result[20] reporting a 48% emission QY in OLAM-treated CdSe NCs. Interestingly, a few other works have reported the reduction in the CdSe photoluminescence upon treatment with amines (see for example Ref. 56). The existence of conflicting observations point to a possibility that treatment with amines may heal certain traps that are not involved in the Z-type displacement. Further research is needed to reconcile these contradictory reports on the emission changes in amine-treated CdSe.

Digestive ripening of CdSe NCs in the OLAM:ODE mixture is likely to cause the displacement of Z-type $Cd(O_2CR)_2$ ligands with L-type OLAM (Fig. 2a), a reaction that was thoroughly investigated by the Owen group.[53,57,56] This process is accompanied by the removal of surface cadmium, which could be detected as a blue–shift of the exciton absorption.[53] Along these expectations, the $1S(h)_{3/2}1S(e)$ excitonic feature of 3.0-nm CdSe NCs was found to blue-shift by about 8 nm (d = 3.0 → 2.85 nm) upon digestive ripening in a OLAM:ODE = 60:40 solution, which corresponds to the loss of about 1/4 monolayer (Fig. 2b). The Z → L displacement scenario was also corroborated by the fact that $2S(h)_{3/2}1S(e)$ excitonic transition, which profile is dependent on the type of surface ligands bound to the nanocrystal,[53] noticeably diminished upon a short exposure to OLAM:ODE = 60:20 at T=180 ˚C (Figs. 2b and SF3). Proton NMR spectra of OLAM-treated CdSe NCs have also confirmed the displacement of original ligands in CdSe with oleylamine, as discussed below (Figs. SF4 and SF5). These surface changes did not seem to affect the lattice bulk structure of CdSe, which, based on the PXRD analysis (Fig. SF6), appeared to be nearly unchanged after 14 hours of DR treatment.

The Z→L ligand displacement during DR appeared reversible, as the addition of $Cd(O_2CR)_2$ to OLAM-treated CdSe (Fig. SF7) partly restored the original position of the CdSe exciton feature (evident from a 6-nm red-shift) while increasing the amplitude of the

$2S_{3/2}(h)1S(e)$ absorbing transition (red arrow, Fig. SF7). It should be noted that the replacement of nanocrystal ligands with n-alkylamines is generally not expected to be 100% efficient unless OA impurities are first etched from the surface.[57] In this regard, the DR-treatment may prove to be an effective tool for the passivation of colloids with a high percentage of L-type surface coverage, as this process is facilitated by the surface ion diffusion and readsorption. Taken all together, the above observations suggest that OLAM-induced DR reaction removes cadmium from Cd-rich nanoparticles leaving NH_2R terminated nanocrystals.

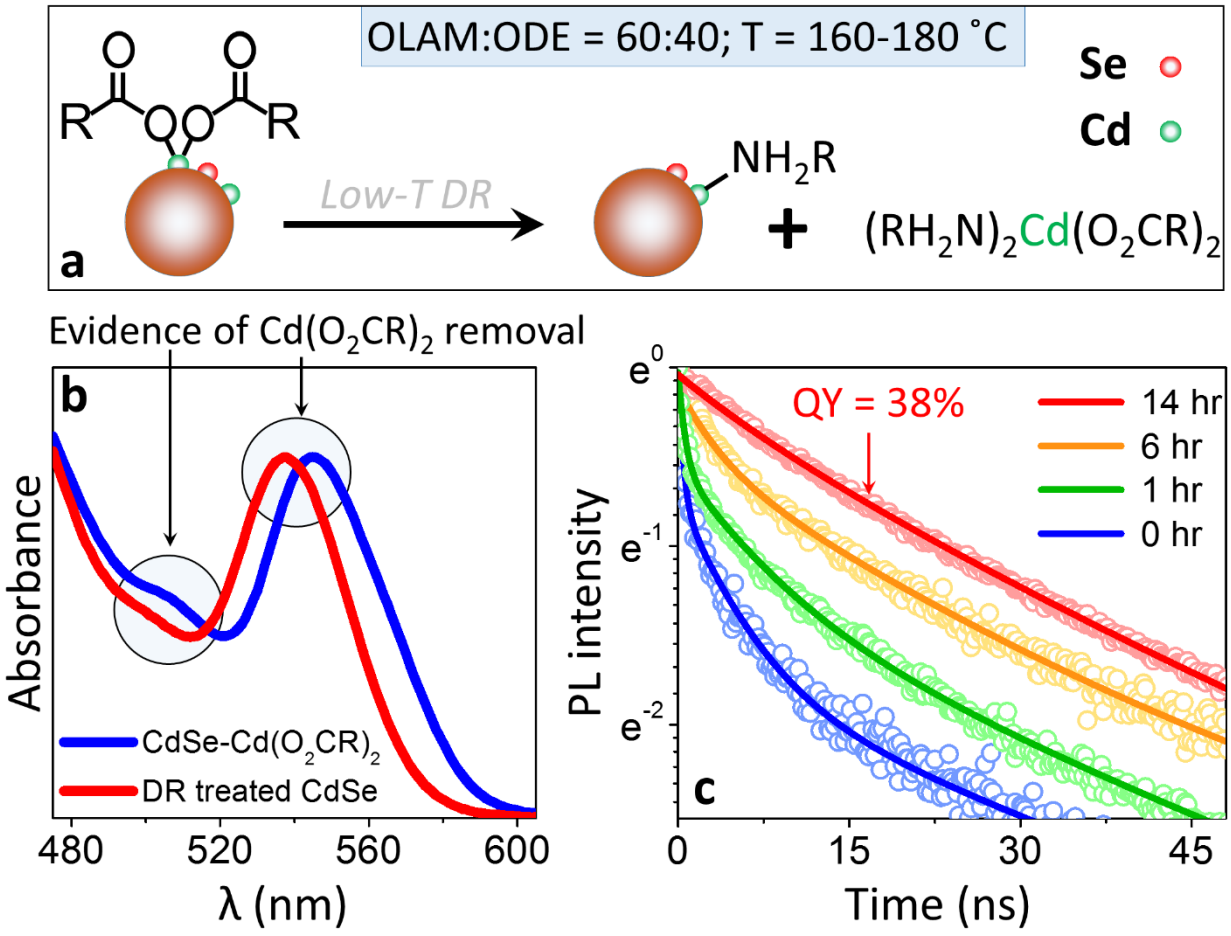

Figure 2. (a). The proposed scheme for the displacement of Z-type ligands with L-type OLAM, which results in the removal of Cd cations from nanocrystal surfaces. (b). Changes in the absorption spectra of 3.0-nm CdSe in the first 20 min of digestive ripening reaction in the OLAM:ODE = 60:40 mixture. The blue-shift of the excitonic absorption feature and the reduced intensity of the $2S(h)_{3/2}1S(e)$ transition are consistent with the removal of Cd cations *via* the Z →

L ligand displacement. During this process, any phosphine ligands on the surface of original nanocrystals are believed to be eventually exchanged with amines. (c). The evolution of the CdSe band gap PL lifetime during the digestive ripening of the two-diameter CdSe sample at T < 180 ˚C. The final sample (14 hours) exhibits the emission QY of 38%.

To further characterize changes in the surface chemistry of CdSe NCs caused by digestive ripening in a OLAM:ODE mixture, we have performed ^{1}H NMR analysis of the nanoparticle sample before and after the DR treatment. To this end, CdSe NCs were first recapped with cadmium oleate (by heating in the presence of octadecene and $CdOA_2$) followed by the redissolution of the purified product in a $CDCl_3$ solvent ($\delta = 7.26$). Figure SF4 compares the ^{1}H NMR spectrum of oleic acid (b) with a CdSe NC dispersion (a). The [CdSe]-$CdOA_2$ NC spectrum features broadened resonances of bound oleate (Fig. SF4b), which were assigned according to previous literature reports as indicated by the insert.[58] As was mentioned above, the exposure of [CdSe]-$CdOA_2$ NCs to OLAM is expected to cause the displacement of cadmium oleate with L-type ligands. This scenario appears to be consistent with the changes observed in the NMR spectra of OLAM treated CdSe NCs (Fig. SF5b,c). In comparison with the resonances of free OLAM (Fig. SF5f), the CdSe-OLAM NC spectra show that all the originally bound oleate resonances lose intensity and acquire a second resonance at lower chemical shift. This observation is exemplified in more detail for the alkene resonance at $\delta = 5.5$ ppm in Fig. SF5a, where the original resonance of the bound oleate can hardly be observed in the [CdSe]-$CdOA_2$ spectrum (Fig. SF5d) due to excessive broadening, but appears to be more distinct upon the OLAM exposure.

It is expected that the DR process can be driven by a variety of free ligands as long as these molecules can efficiently solubilize ions and monomers in the growth solution. To test this hypothesis, OLAM was replaced with oleic acid as a DR initiating agent. The dynamics of CdSe NC shape evolution during the DR reaction in the presence of OA was investigated by monitoring the absorption profile of a mixed CdSe NC sample containing two different particle sizes (d = 2.1 and d = 2.6 nm). The temperature of the OA:ODE = 70:30 reaction mixture was kept below 170 ˚C to suppress interparticle coalescence. According to Fig. 3a, the absorption features of the two nanocrystal types gradually converge into a single peak upon heating, consistent with the reduction in the particle size dispersion. Similarly to the case of OLAM-induced ripening, the employment of a OA:ODE reaction mixture allowed reducing the standard deviation of CdSe sizes from 22% to about 5-6% in 10 hours.

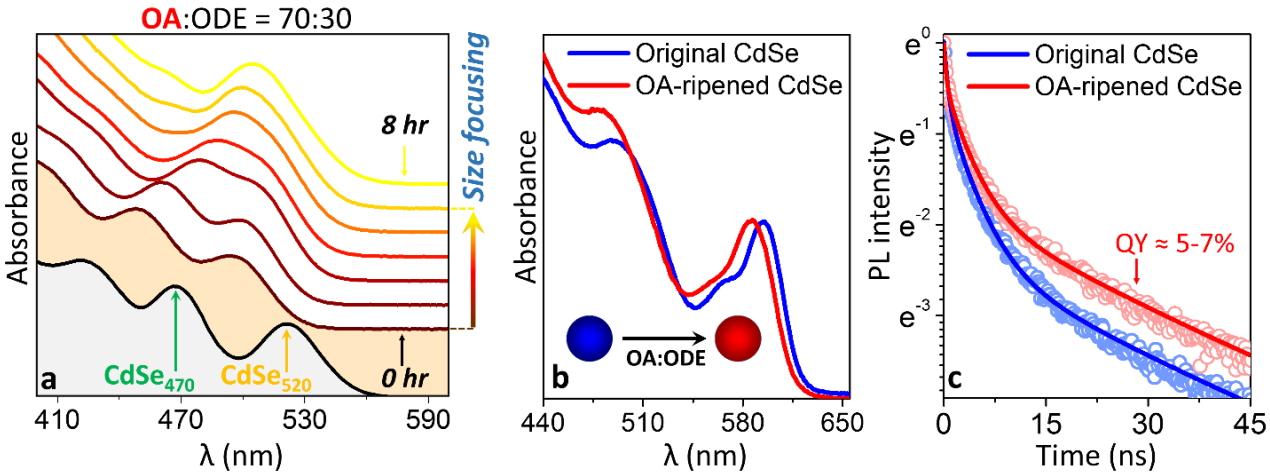

Figure 3. (a). Oleic acid-induced digesting ripening of a $CdSe_{470}$ + $CdSe_{520}$ nanocrystal mixture containing two sizes of CdSe nanocrystals (d = 2.1 nm and d = 2.6 nm). The associated low-energy absorbing transitions in the starting sample are labelled with a green and yellow dashed lines. Heating of the polydispersed nanoparticle sample in the OA:ODE = 70:30 reaction mixture at T ≤ 170 ˚C resulted in a gradual convergence of the two absorbing features into a single profile, corresponding to the reduction in the particle size dispersion from 22% to about 5-6%. (b). Changes in the absorption spectra of CdSe NCs in the first 20 min of digestive ripening

reaction in the OA:ODE = 70:30 mixture. (c). The evolution of the CdSe band gap PL lifetime during the digestive ripening reaction at 170 ˚C. The 10-hour sample exhibited the emission QY of 5-7%.

Digestive ripening of CdSe NCs in a OA:ODE solution was expected to produce rather complex changes in the nanoparticle surface chemistry made possible by the diffusion and reabsorption of ligated surface ions and monomers. Considering that the replacement of Z-type and L-type (TOP) ligands in original CdSe NCs with an X-type OA would require a change in the surface charge, one can expect this process to be accompanied by changes in the surface cation-to-anion ratio. Indeed, for the surface charge neutrality of CdSe NCs to be preserved upon binding of electron-donating X-type OA (donating a -1 charge to the bond) to surfaces L-type passivated nanocrystals (contributing zero surface charge), the proportion of negative ions on the surface should be reduced. This could be achieved though the addition of metal cations or removal of anions. The former appears to be less likely since no Cd precursors are introduced during the DR procedure.

To explore whether surface anions are removed during digestive ripening of CdSe NCs to balance the charge of oleic acid ligands, we first examine the evolution of the exciton absorption in 4.1-nm CdSe NCs caused by the DR treatment at T = 170 ˚C. According to Figs. 3b and SF8b, the DR reaction in a OA:ODE = 70:30 mixture results in a blue shift of the exciton feature by 5-10 nm, which supports the ion removal hypothesis. These absorption changes could not be reversed by the addition of $Cd(OA)_2$ as evidenced from the absence of a red-shift in Fig. SF8a, which is consistent with Cd-rich surfaces of OA-treated CdSe NCs due to removal of Se.

To further characterize the stoichiometric changes accompanying the ligand exchange processes for OA- and OLAM-treated CdSe samples, we have performed the energy dispersive X-ray (EDX) analysis of nanoparticle elemental compositions for each case. To this end, a Cd:Se X-ray emission ratio in original CdSe NCs ($r \approx 1.75$), obtained by integrating the area of the Se_L and Cd_L x-ray emission peaks in Fig. 4a (red curve), was compared to Cd:Se ratios in DR-treated

nanoparticles. According to Fig. 4a, the digestive ripening in OLAM reduces the Cd:Se ratio in nanocrystals (r ≈1.51), which supports the proposed of Z to L ligand displacement (loss of Cd). Conversely, when the DR reaction is performed in OA solutions, the ratio of the Cd to Se atoms becomes slightly increased in the final nanoparticle product (r ≈ 1.97), suggesting that Se is in fact being removed from nanoparticle surfaces. The absolute changes in the Cd:Se ratio are fairly small as these represent contributions from surface and bulk atoms. Considering that the average diameter of investigated CdSe NC sample is 4.1 nm, we estimate that the fraction of surface atoms amounts to ~30%. Overall, the EDX measurements support the hypothesis that OLAM solutions remove Cd while OA solutions remove Se (see Fig. 4c).

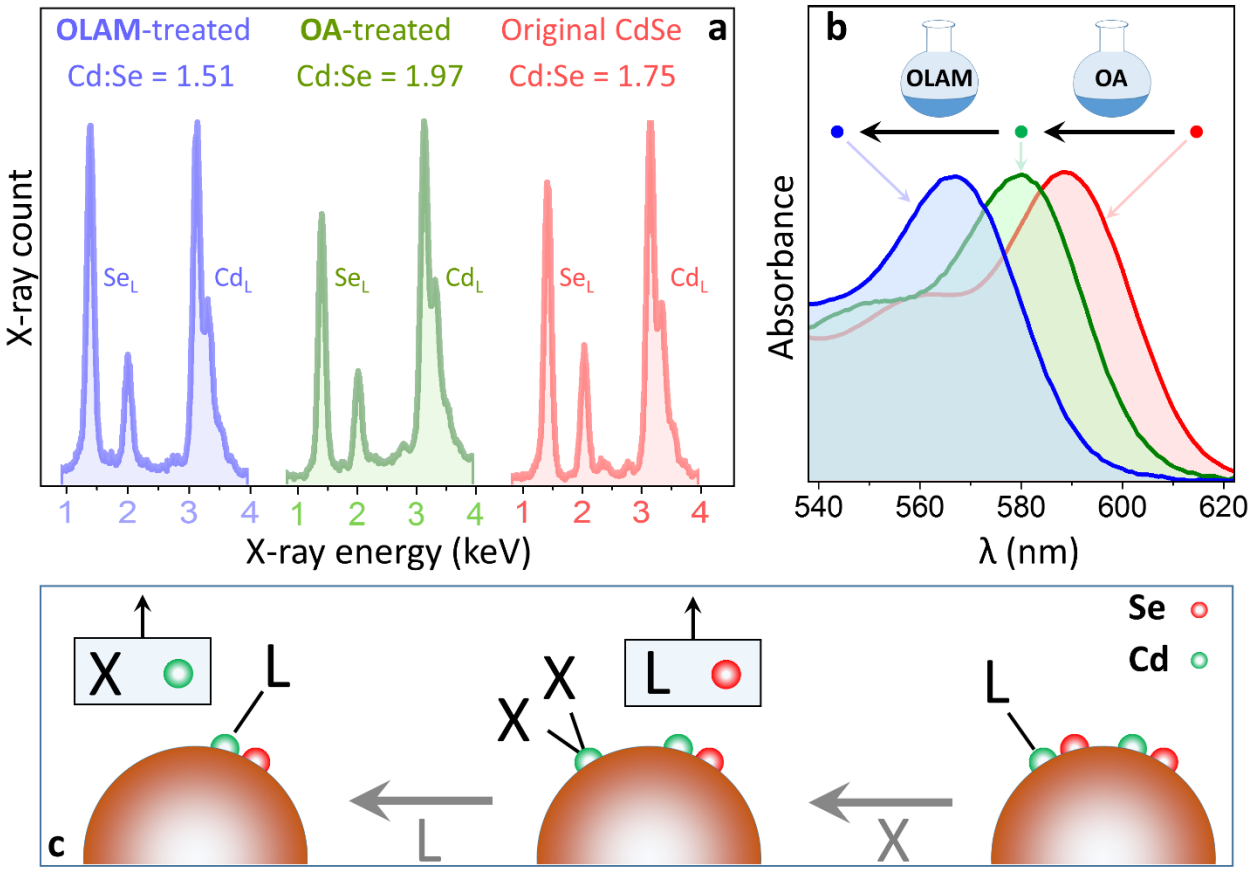

Figure 4. (a). Energy dispersive X-ray characterization of the elemental composition for CdSe NCs ripened in OLAM (blue) and OA (green). The EDX of original CdSe NCs is shown in red. The observed changes in the Cd:Se X-ray emission ratios supports the hypothesis that DR

processes in OLAM and OA solutions result in a loss of surface Cd and Se ions, respectively. (b). Changes in the exciton absorption of 4.1-nm CdSe NCs accompanied by the consecutive application of OA and OLAM digestive ripening treatments (T ≈ 150-170 ˚C). The total spectral blue-shift resulting from both applications corresponds to the 0.6-nm loss in the average particle diameter. (c). The proposed scheme of surface ligand exchanges in CdSe NCs corresponding to a consecutive application of OA and OLAM DR treatments.

The desorption of surface ions to balance the charge of incoming ligands in CdSe NCs can be observed directly through a consecutive application of OLAM and OA digestive ripening treatments. Figure 4b summarizes the changes in the absorption profile of 4.1-nm CdSe NCs upon the exposure of these nanoparticles to ODE:OA = 30:70 solutions at 160 ˚C, followed by a single wash with ethanol, and the subsequent exposure to a 70% OLAM solution in ODE at 160 ˚C. Each of the two DR processes resulted in a blue-shift of the exciton absorption feature by 10-15 nm. The total blue shift of $\lambda = 25$ nm corresponds to the 0.6-nm reduction in the diameter of original nanocrystals, which is equivalent to nearly a full CdSe monolayer. Similar dynamics was observed for 3.2-nm CdSe (see Fig. SF9) where a reverse application of consecutive OLAM and OA DR processes (T < 150 ˚C) resulted in 0.15-nm reduction in the nanocrystal diameter.

To understand whether digestive ripening represents a feasible size focusing strategy for other semiconductor colloids, we have applied low-temperature DR to samples of ZnSe NCs. The shape of these nanocrystals is notoriously difficult to control due to the competition of zinc blende and wurtzite polymorphs that tend to form multibranched structures.[45,59,60] Previous successful attempts to synthesize uniform particles of ZnSe have relied on well executed strategies utilizing carefully balanced precursors.[61,62] Here, we explore a general approach to uniform ZnSe NCs that benefits from the simplicity of the DR procedure. To this end, polydisperse ZnSe NCs were first synthesized using known protocols[45] comprising a TOP/ODA ligand combination. The TEM image of the product in Figs. 5a and 5b reveals commonly

observed branching of ZnSe nanostructures. Following a single wash with ethanol, the product was redispersed in OLAM:ODE = 70:30 solution and heated up to 170 ˚C. After 5 hours of the DR reaction, apparent focusing of nanoparticle shapes was observed (Fig. 5c), manifested by predominantly spherically shaped nanoparticles. Same digestive ripening conditions applied using a higher concentration of the original ZnSe seeds have resulted in the growth of nanorod-shaped structures.

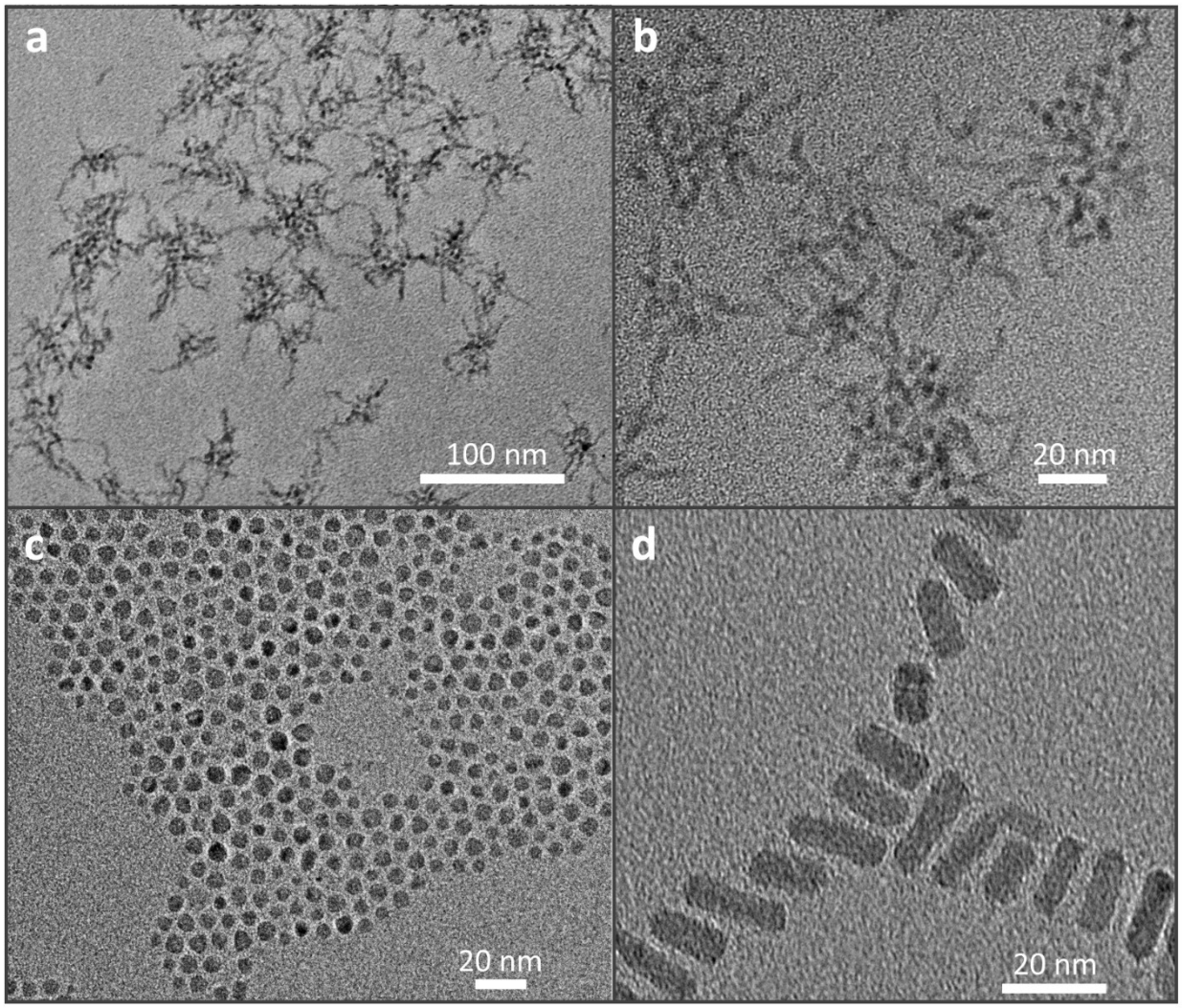

Figure 5. (a,b). Transmission Electron Microscope (TEM) images of as-synthesized ZnSe nanocrystals exhibiting a commonly observed branched morphology. (c). TEM image of approximately spherical ZnSe NCs obtained after applying the digestive ripening treatment to as-

fabricated product in (a) for 5 hours in a OLAM:ODE = 70:30 solution (low seed concentration). (d). Nanorod-shaped ZnSe NCs obtained from the as-fabricated product in (a) by applying the digestive ripening treatment for 5 hours in a OLAM:ODE = 80:20 solution (high seed concentration)

CONCLUSIONS

In conclusion, we demonstrate that digestive ripening of colloidal semiconductor nanocrystals represents a viable post-synthetic strategy for tuning the surface-ligand chemistry and reducing the particle size dispersion. This process employs highly concentrated ligand solutions to promote two concurrent mechanisms: (*i*) - the diffusion of nanocrystal ions into the solvent, which accelerates an interparticle ion exchange across nanocrystal populations, and (*ii*) - thermally activated interparticle coalescence, which leads to the nanoparticle growth. We show that the latter process can be fully suppressed by working in a low temperature regime, which leads to diffusion-driven focusing of nanoparticle shapes and sizes. In this work, the size-focusing effect of low-temperature digestive ripening was demonstrated using a mixed sample of CdSe NCs featuring two different particle diameters (2.1 and 2.6 nm). The application of digesting ripening resulted in a gradual convergence the two CdSe sizes into one (2.45 nm) corresponding to the four-fold reduction in the particle size dispersion. Size focusing was found to be similarly effective with either L-type (oleylamine) or X-type (oleic acid) DR-initiating ligands. The technique was subsequently adapted to achieve size focusing in samples of ZnSe NCs leading to enhanced homogeneity of nanoparticle shapes. Digestive ripening was also shown to facilitate complex ligand exchange processes that require restructuring of nanocrystal surfaces. In particular, the enhanced diffusion of surface ions during the digestive ripening reaction has been shown to promote a classically forbidden L $\rightarrow$ X ligand exchange in CdSe

NCs, which was possible due to the desorption of surface Se. Overall, we expect that the DR approach could be extended to many semiconductor materials as a simple tool for controlling the surface chemistry and reducing the size dispersion of colloidal nanostructures.

Supporting information. Experimental section, ^{1}H NMR spectra, UV/Vis data, and details of calculation. This material is available free of charge via the Internet at http://pubs.acs.org.

Acknowledgments. We gratefully acknowledge NSF Award DMR-1710063 for financial support. PM was supported in part by CHE-1465052 Award.

REFERENCES

[1] Murray, C. B.; Norris, D. J.; Bawendi, M. G. Synthesis and Characterization of Nearly Monodisperse CdE (E = Sulfur, Selenium, Tellurium) Semiconductor Nanocrystallites. *J. Am. Chem. Soc.* **1993**, *115*, 8706–8715.

[2] Kovalenko, M. V.; Manna, L.; Cabot, A.; Hens, Z.; Talapin, D. V.; Kagan, C. R.; Klimov, V. I.; Rogach, A. L.; Reiss, P.; Milliron, D. J.; Guyot-Sionnnest, P.; Konstantatos, G.; Parak, W.J.; Hyeon, T.; Korgel, B. A.; Murray, C. B.; Heiss, W. Prospects of Nanoscience with Nanocrystals. *ACS Nano* **2015**, *9*, 1012–1057.

[3] Lim, J.; Park, Y-S.; Klimov, V. I. Optical Gain in Colloidal Quantum Dots Achieved with Direct-Current Electrical Pumping. *Nat. Mater.* **2018**, *17*, 42–49.

[4] Mashford, B. S.; Stevenson, M.; Popovic, Z.; Hamilton, C.; Zhou, Z.; Breen, C.; Steckel, J.; Bulovic, V.; Bawendi, M. G.; Coe-Sullivan S.; Kazlas, P. T. High-Efficiency Quantum-Dot Light-Emitting Devices with Enhanced Charge Injection. *Nat. Photonics* **2013**, *7*, 407-412.

[5] Beard, M.C.; Blackburn, J. L.; Johnson, J. C.; Rumbles, G. Status and Prognosis of Future Generation Photoconversion to Photovoltaics and Solar Fuels. *ACS Energy Lett*. **2016**, *1*, 344–347.

[6] Ko, D. K.; Maurano, A.; Suh, S. K.; Kim, D.; Hwang, G.W.; Grossman, J. C.; Bulovic, V.; Bawendi, M. G. Photovoltaic Performance of PbS Quantum Dots Treated with Metal Salts. *ACS Nano* **2016**, *10*, 3382–3388.

[7] Yang, Z.; Fan, J. Z.; Proppe, A. H.; Pelayo García de Arquer, F.; Rossouw, D.; Voznyy, O.; Lan, X.; Liu, M.; Walters, G.; Quintero-Bermudez, R.; Sun, B.; Hoogland, S.; Botton, G. A.; Kelley, S. O.; Sargent, E. H. Mixed-Quantum-Dot Solar Cells. *Nat. Commun.* **2017**, *8*, 1325.

[8] Medintz, I. L.; Pons, T.; Boeneman, K.; Susumu, K.; Deschamps, J. R.; Farrell, D.; Melinger, J. S.; Dennis, A. M.; Bao, G.; Mattoussi, H. Resonance Energy Transfer Between Luminescent Quantum Dots and Diverse Fluorescent Protein Acceptors. *J. Phys. Chem. C* **2009**, *113*, 18552-18561.

[9] Boulesbaa, A.; Huang, Z.; Wu, D.; Lian, T. Competition between Energy and Electron Transfer from CdSe QDs to Adsorbed Rhodamine B. *J. Phys. Chem. C* **2010**, *114*, 962–969.

[10] Razgoniaeva, N.; Moroz, P.; Lambright, S.; Zamkov, M. Photocatalytic Applications of Colloidal Heterostructured Nanocrystals: What's Next? *J. Phys. Chem. Lett.* **2015**, *6*, 4352-4359.

[11] Chen, S.; Takata, T.; Domen, K. Particulate Photocatalysts for Overall Water Splitting. *Nat. Rev. Mater.* **2017**, *2*, 17050.

[12] Boles, M. A.; Engel, M.; Talapin, D. V. Self-Assembly of Colloidal Nanocrystals: From Intricate Structures to Functional Materials. *Chem. Rev.* **2016**, *116*, 11220-11289.

[13] Chandler, R. E.; Houtepen, A. J.; Nelson, J.; Vanmaekelbergh, D. Electron Transport in Quantum Dot Solids: Monte Carlo Simulations of the Effects of Shell Filling, Coulomb Repulsions, and Site Disorder. *Phys. Rev. B* **2007**, *75*, 085325.

[14] Gilmore, R. H.; Lee, E. M. Y.; Weidman, M. C.; Willard, A. P.; Tisdale, W. A. Charge Carrier Hopping Dynamics in Homogeneously Broadened PbS Quantum Dot Solids. *Nano Lett.* **2017**, *17*, 893-901.

[15] Park, J.; Joo, J.; Kwon, S. G.; Jang, Y.; Hyeon, T. Synthesis of Monodisperse Spherical Nanocrystals. *Angew. Chem. Int. Ed.* **2007**, *46*, 4630–4660.

[16] Razgoniaeva, N.; Carrillo, L.; Burchfield, D.; Moroz, P.; Adhikari, P.; Yadav, P.; Khon, D.; Zamkov, M. Colloidal Synthesis of Monodisperse Semiconductor Nanocrystals through the Saturated Ionic Layer Adsorption. *Chem. Mater.* **2016**, *28*, 2823-2833.

[17] Dai, Q.; Wang, Y.; Li, X.; Zhang, Y.; Pellegrino, D. J.; Zhao, M.; Zou, B.; Seo, J.; Wang, Y.; Yu, W. W. Size-Dependent Composition and Molar Extinction Coefficient of PbSe Semiconductor Nanocrystals. *ACS Nano* **2009**, *3*, 1518−1524.

[18] Morris-Cohen, A. J.; Frederick, M. T.; Lilly, G. D.; Mcarthur, E. A.; Weiss, E. A. Organic Surfactant Controlled Composition of the Surfaces of CdSe Quantum Dots. *J. Phys. Chem. Lett.* **2010**, *1*, 1078−1081.

[19] Smith, D. K.; Luther, J. M.; Semonin, O. E.; Nozik, A. J.; Beard, M. C. Tuning the Synthesis of Ternary Lead Chalcogenide Quantum Dots by Balancing Precursor Reactivity. *ACS Nano* **2011**, *5*, 183−190.

[20] Chen, O.; Yang, Y. A.; Wang, T.; Wu, H. M.; Niu, C. G.; Yang, J. H.; Cao, Y. C. Surface-Functionalization-Dependent Optical Properties of II-VI Semiconductor Nanocrystals. *J. Am. Chem. Soc.* **2011**, *133*, 17504−17512.

[21] Hassinen, A.; Moreels, I.; De Nolf, K.; Smet, P. F.; Martins, J. C.; Hens, Z. Short-Chain Alcohols Strip X-Type Ligands and Quench the Luminescence of PbSe and CdSe Quantum Dots, Acetonitrile Does Not. *J. Am. Chem. Soc.* **2012**, *134*, 20705−20712.

[22] Munro, A. M.; Ginger, D. S. Photoluminescence Quenching of Single CdSe Nanocrystals by Ligand Adsorption. *Nano Lett.* **2008**, *8,* 2585−2590.

[23] Peng, X. G.; Wickham, J.; Alivisatos, A. P. Kinetics of II-VI and III-V Colloidal Semiconductor Nanocrystal Growth: "Focusing" of Size Distributions. *J. Am. Chem. Soc.* **1998**, *120*, 5343-5344.

[24] Talapin, D. V.; Rogach, A. L.; Kornowski, A.; Haase, M.; Weller, H. Highly Luminescent Monodisperse CdSe and CdSe/ZnS Nanocrystals Synthesized in a Hexadecylamine-Trioctylphosphine Oxide-Trioctylphospine Mixture. *Nano Lett.* **2001**, *1*, 207–211.

[25] Hines, M. A.; Scholes, G. D. Colloidal PbS Nanocrystals with Size-Tunable Near-Infrared Emission: Observation of Post-Synthesis Self-Narrowing of the Particle Size Distribution. *Adv. Mater.* **2003**, *15*, 1844–1849.

[26] Donega, C. D.; Hickey, S. G.; Wuister, S. F.; Vanmaekelbergh, D.; Meijerink, A. Single-Step Synthesis to Control the Photoluminescence Quantum Yield and Size Dispersion of CdSe Nanocrystals. *J. Phys. Chem. B* **2003**, *107*, 489−496.

[27] Greytak, A. B.; Tan, R.; Roberts, S. K. Prospects for Rational Control of Nanocrystal Shape Through Successive Ionic Layer Adsorption and Reaction (SILAR) and Related Approaches. In: *Anisotropic and Shape-Selective Nanomaterials. Nanostructure Science and Technology*; Hunyadi Murph, S. E.; Larsen, G.; Coopersmith, K., Eds. Springer: Cham, Switzerland; 2017, 169-232.

[28] Rempel, J. Y.; Bawendi, M. G.; Jensen, K. F. Insights into the Kinetics of Semiconductor Nanocrystal Nucleation and Growth. *J. Am. Chem. Soc.* **2009**, *131*, 4479–4489.

[29] Lifshitz, I.; Slyozov, V. J. The Kinetics of Precipitation from Supersaturated Solid Solutions. *Phys. Chem. Solids*. **1961**, *19*, 35-50.

[30] Ostwald, W. Z. *Phys. Chem. Stoechiom. Verwandtschaftsl.* **1900**, *34*, 495-503.

[31] Watzky, M. A.; Finke, R. G. Nanocluster Size-Control and "Magic Number" Investigations. Experimental Tests of the "Living-Metal Polymer" Concept and of Mechanism-Based Size-Control Predictions Leading to the Syntheses of Iridium(0) Nanoclusters Centering about Four Sequential Magic Numbers. *Chem. Mater*. **1997**, *9*, 3083-3095.

[32] Razgoniaeva, N.; Acharya, A.; Sharma, N.; Adhikari, P.; Shaughnessy, M.; Moroz, P.; Khon, D.; Zamkov, M. Measuring the Time-Dependent Monomer Concentration During the Hot-Injection Synthesis of Colloidal Nanocrystals. *Chem. Mater*. **2015**, *27*, 6102-6108.

[33] Cingarapu, S.; Yang, Z.; Sorensen, C. M.; Klabunde, K. J. Synthesis of CdSe/ZnS and CdTe/ZnS Quantum Dots: Refined Digestive Ripening. *J. Nanomater.* **2012**, *312087*, 1−12.

[34] Cingarapu, S.; Yang, Z.; Sorensen, C. M.; Klabunde, K. J. Synthesis of CdSe Quantum Dots by Evaporation of Bulk CdSe Using SMAD and Digestive Ripening Processes. *Chem. Mater*. **2009**, *21*, 1248–1252

[35] Lin, X. M.; Sorensen, C. M.; Klabunde, K. J. Digestive Ripening, Nanophase Segregation and Superlattice Formation in Gold Nanocrystal Colloids. *J. Nanopart. Res.* **2000**, *2*, 157−164.

[36] Polte, J.; Ahner, T. T.; Delissen, F.; Sokolov, S.; Emmerling, F.; Thunemann, A. F.; Kraehnert, R. Mechanism of Gold Nanoparticle Formation in the Classical Citrate Synthesis Method

Derived from Coupled In Situ XANES and SAXS Evaluation. *J. Am. Chem. Soc.* **2010**, *132*, 1296-1301.

[37] Sahu, P.; Prasad, B. L. V. Fine Control of Nanoparticle Sizes and Size Distributions: Temperature and Ligand Effects on the Digestive Ripening Process. *Nanoscale* **2013**, *5*, 1768−1771.

[38] Wang, J.; Boelens, H. F. M.; Thathagar, M. B.; Rothenberg, G. *In Situ* Spectroscopic Analysis of Nanocluster Formation. *ChemPhysChem* **2004**, *5*, 93-98.

[39] Nishimura, S.; Takagaki, A.; Maenosono, S.; Ebitani, K. *In Situ* Time-Resolved XAFS Study on the Formation Mechanism of Cu Nanoparticles Using Poly(N-vinyl-2-pyrrolidone) as a Capping Agent. *Langmuir* **2009**, *26*, 4473-4479.

[40] Seth, J.; Prasad, B. L. V. Bromide Ion Mediated Modification to Digestive Ripening Process: Preparation of Ultra-Small Pd, Pt, Rh and Ru Nanoparticles. *Nano Res.* **2016**, *9*, 2007-2017.

[41] Razgoniaeva, N.; Yang, M.; Garrett, P.; Kholmicheva, N.; Moroz, P.; Eckard, H.; Royo Romero, L.; Porotnikov, D.; Khon, D.; Zamkov, M. Just Add Ligands: Self-Sustained Size Focusing of Colloidal Semiconductor Nanocrystals. *Chem. Mater*. **2018**, *30*, 1391-1398.

[42] Zhou, Y.; Buhro, W. E. Reversible Exchange of L-Type and Bound-Ion-Pair X-Type Ligation on Cadmium Selenide Quantum Belts. *J. Am. Chem. Soc.* **2017**, *139*, 12887−12890.

[43] Carbone, L.; Nobile, C.; De Giorgi, M.; Della Salla, F.; Morello, G.; Pompa, P.; Hytch, M.; Snoeck, E.; Fiore, A.; Franchini, I. R.; Nadasan, M.; Silvestre, A. F.; Chiodo, L.; Kudera, S.; Cingolani, R.; Krahne, R.; Manna, L. Synthesis and Micrometer-Scale Assembly of Colloidal CdSe/CdS Nanorods Prepared by a Seeded Growth Approach. *Nano Lett.* **2007***, 7*, 2942-2950.

[44] Peng, Z. A.; Peng, X. G. Nearly Monodisperse and Shape-Controlled CdSe Nanocrystals via Alternative Routes: Nucleation and Growth. *J. Am. Chem. Soc*. **2002**, *124*, 3343-3353.

[45] Cozzoli, P. D.; Manna, L.; Curri, M. L.; Kudera, S.; Giannini, C.; Striccoli, M.; Agostiano, A. Shape and Phase Control of Colloidal ZnSe Nanocrystals. *Chem. Mater.*, **2005**, *17*, 1296–1306.

[46] Jadzinsky, P. D.; Calero, G.; Ackerson, C. J.; Bushnell, D. A.; Kornberg, R. D. Structure of a Thiol Monolayer-Protected Gold Nanoparticle at 1.1 Å Resolution. *Science* **2007**, *318*, 430−433.

[47] Hakkinen, H. The Gold-Sulfur Interface at the Nanoscale. *Nat. Chem.* **2012**, *4*, 443-455.

[48] Biener, M. M.; Biener, J.; Friend, C. M. Revisiting the S−Au(111) Interaction: Static or Dynamic? *Langmuir* **2005**, *21*, 1668−1671.

[49] Shimpi, J.R.; Sidhaye, D.S.; Prasad, B.L.V. Digestive Ripening: A Fine Chemical Machining Process on the Nanoscale. *Langmuir* **2017**, *33*, 9491–9507.

[50] Lee, D.-K.; Park, S-I.; Lee, J. K.; Hwang, N. M. A Theoretical Model for Digestive Ripening. *Acta Mater.* **2007**, *55*, 5281–5288.

[51] Shen, Y.; Tan, R.; Gee, M. Y.; Greytak, A. B. Quantum Yield Regeneration: Influence of Neutral Ligand Binding on Photophysical Properties in Colloidal Core/Shell Quantum Dots. *ACS Nano* **2015**, *9*, 3345-3359.

[52]Yu, W.; Qu, L.; Guo, W.; Peng, X. Experimental Determination of the Extinction Coefficient of CdTe, CdSe, and CdS Nanocrystals. *Chem. Mater.* **2003**, *15*, 2854–2860.

[53] Anderson, N. C.; Owen, J. S. Soluble, Chloride-Terminated CdSe Nanocrystals: Ligand Exchange Monitored by ^{1}H and ^{31}P NMR Spectroscopy. *Chem. Mater.* **2013**, *25*, 69−76.

[54]Ji, X.; Copenhaver, D.; Sichmeller, C.; Peng, X. Ligand Bonding and Dynamics on Colloidal Nanocrystals at Room Temperature: The Case of Alkylamines on CdSe Nanocrystals. *J. Am. Chem. Soc*. **2008**, *130*, 5726–5735.

[55] Saniepay, M.; Mi, C.; Liu, Z.; Abel, E. P.; Beaulac, R. Insights into the Structural Complexity of Colloidal CdSe Nanocrystal Surfaces: Correlating the Efficiency of Nonradiative Excited-State Processes to Specific Defects. *J. Am. Chem. Soc.* **2018**, *140*, 1725−1736.

[56] Anderson, N. C.; Hendricks, M. P.; Choi, J.; Owen, J. S. Ligand Exchange and the Stoichiometry of Metal Chalcogenide Nanocrystals: Spectroscopic Observation of Facile Metal-Carboxylate Displacement and Binding. *J. Am. Chem. Soc.* **2013**, *135*, 18536−18548

[57] Chen, P. E.; Anderson, N. C.; Norman, Z. M.; Owen, J. S. Tight Binding of Carboxylate, Phosphonate, and Carbamate Anions to Stoichiometric CdSe Nanocrystals. *J. Am. Chem. Soc*. **2017**, *139*, 3227−3236.

[58] Fritzinger, B.; Capek, R. K.; Lambert, K.; Martins, J. C.; Hens, Z. Utilizing Self-Exchange to Address the Binding of Carboxylic Acid Ligands to CdSe Quantum Dots. *J. Am. Chem. Soc.* **2010**, *132*, 10195−201.

[59]Omata, T.; Uesugi, H.; Kita, M. Phase Determination of Zinc Selenide Nanocrystals Depending on the Ligand Species of Precursor Complexes. *J. Cryst. Growth* **2014**, *394*, 81-88.

[60] Jia, G.; Banin, U. A General Strategy for Synthesizing Colloidal Semiconductor Zinc Chalcogenide Quantum Rods. *J. Am. Chem. Soc*. **2014**, *136*, 11121–11127.

[61] Hines, M. A.; Guyot-Sionnest, P. J. Bright UV-Blue Luminescent Colloidal ZnSe Nanocrystals. *Phys. Chem. B* **1998**, *102*, 3655-3657.

[62] Shavel, A.; Gaponik, N.; Eychmuller, A. Efficient UV-Blue Photoluminescing Thiol-Stabilized Water-Soluble Alloyed ZnSe(S) Nanocrystals. *J. Phys. Chem. B* **2004**, *108*, 5905-5908.